Available online at www.sciencedirect.com
SCIENCE DIRECT
Journal of Photochemistry and Photobiology A: Chemistry 179 (2006) 135–141
Journal of Photochemistry and Photobiology A:Chemistry
www.elsevier.com/locate/jphotochem

Synthesis of size-controlled CdSe quantum dots and characterization of CdSe–conjugated polymer blends for hybrid solar cells

Sang-Hyun Choi [a], Hongju Song [b], Il Kyu Park [b], Jun-Ho Yum [b], Seok-Soon Kim [b], Seonghoon Lee [c], Yung-Eun Sung [a,*]

[a] *Interdiciplinary Program of Nano-science and Technology and School of Chemical & Biological Engineering, Seoul National University, Seoul 151-744, Republic of Korea*
[b] *Department of Materials Science and Engineering, Gwangju Institute of Science and Technology (GIST), Gwangju 500-712, Republic of Korea*
[c] *Department of Chemistry and Molecular Engineering, Seoul National University, Seoul 151-747, Republic of Korea*

Received 6 May 2005; received in revised form 3 July 2005; accepted 2 August 2005
Available online 6 September 2005

Abstract

High-quality CdSe quantum dots (Qdots) were produced using the wet chemical synthetic method. These size-controlled CdSe Qdots were characterized by UV–vis absorption spectroscopy, photoluminescence (PL) spectroscopy, Fourier transform infrared spectroscopy (FT-IR), X-ray diffraction (XRD), X-ray photoelectron spectroscopy (XPS), scanning electron microscopy (SEM) and transmission electron microscopy (TEM). The XRD patterns and TEM images showed that the CdSe Qdots had a wurtzite crystalline structure. Bandgap-tuning CdSe Qdots were used to fabricate solar cells. We report the extensive experimental results of the CdSe Qdots–conjugated polymer composites used for the fabrication of the hybrid solar cells, by blending them between CdSe Qdots–poly (3-hexylthiophene) (P3HT) and CdSe Qdots/[poly(1-methoxy-4-(2-ethylhexyloxy-2,5-phenylenevinylene))] (MEH-PPV) polymer.

Keywords: CdSe quantum dots (Qdots); Conjugated polymer; Hybrid solar cells

1. Introduction

Recently, a composite consisting of semiconductor nanocrystals and an organic polymer have attracted considerable attention in the field of solar cells, because of their having no harmful effects on the environment. Such organic materials have the many advantages, such as low cost, large processing, flexible compatibility and the use of a light-weight plastic substrate [1–4]. However, due to their low charge carrier mobility and short exciton diffusion length, the solar energy conversion efficiencies of these devices are very low. In order to improve their efficiency, these photovoltaic devices require the introduction of other materials in order to promote electron transport. However, when introducing other organic materials, the interface required for charge transfer should be taken into consideration [5,6]. Therefore, for this purpose, inorganic compounds are often blended with the polymers at an appropriate concentration in order to promote the formation of percolation pathways for charge transport [7–9]. Alivisatos and co-workers [5,6,10,11] reported that one way to overcome these charge transport limitations is to blend the polymer with inorganic semiconductor nanocrystals.

Herein, we report on the synthesis of size-controlled CdSe quantum dots (Qdots) [12] using the wet chemical synthetic method and their subsequent blending CdSe Qdots with the polymer. Moreover, this paper focuses particularly on the characterization using the size-controlled CdSe Qdots. Finally, we report our experimental results concerning the blending of the composites for the purpose of fabricating a hybrid solar cell [5,6] based on the conjugated polymers. The example given is the blending of regioregular poly (3-hexylthiophene) (P3HT) polymer, [poly(1-methoxy-4-(2-

* Corresponding author. Tel.: +82 2 880 1889; fax: +82 2 888 1604.
E-mail address: ysung@snu.ac.kr (Y.-E. Sung).

1010-6030/$ – see front matter © 2005 Elsevier B.V. All rights reserved.
doi:10.1016/j.jphotochem.2005.08.004

ethylhexyloxy-2,5-phenylenevinylene))] (MEH-PPV) polymer, and the CdSe Qdots, while tuning their size. In these polymer–Qdots composites [13], when the nanocrystals surface is not coated with trioctylphosphine oxide (TOPO) but other surfactants [14], we found the photoluminescence (PL) quenching and charge transfer occurred at the polymer–Qdots interface. The morphology of composite materials is also presented in detail, based on their optical and structural characterization with PL, AFM, scanning electron microscopy (SEM) and transmission electron microscopy (TEM).

2. Experimental

2.1. Materials

Trioctylphosphine oxide (TOPO, 90%) and triocytlphosphine (TOP, 95%) were obtained from Strem and Fluka, respectively. Selenium powder (99.999%) was purchased from Aldrich and P3HT polymer from Aldrich was purified by Soxhlet extraction. MEH-PPV polymer was yielded by the base-induced polymerization of 2,5-bis(chloromethyl)-1-methoxy-4-(2-ethylhexyloxy)benzene in THF [15]. Dimethylcadmium (Me_2Cd, 99.99%) was purchased from Strem and was filtered separately through a 0.2 μm filter in an inert glove box. A 1.0 M stock solution of TOPSe was prepared by dissolving selenium powder in TOP. Hexane was purchased from Junsei. Methanol, pyridine and *n*-butanol were purchased from Merck.

2.2. Synthesis of CdSe quantum dots

CdSe Qdots ranging in diameter from 2.4 to 5.5 nm were synthesized using the wet chemical synthetic method as the modified synthesis [12]. The TOP/TOPO-capped CdSe Qdots were synthesized as follows; trioctylphosphine oxide (90%) was dried and degassed in the reaction flask by heating it to 180 °C under 200 mTorr of N_2 for 20 min, periodically. The temperature of the reaction flask was then slowly increased up to 350 °C under 1 atm of N_2. A stock solution of Cd and Se precursors was prepared by adding the known equivalent-molar amounts of Me_2Cd and 1 M TOPSe to TOP in an N_2-filled glove box and a sample was then loaded into a syringe. The syringe containing the reagent mixture was quickly removed from the glove box and its contents injected into the vigorously stirred reaction flask quickly through a rubber septum. We were able to control the final size of the CdSe Qdots by varying the concentration of the Cd, Se precursors, while maintaining the TOPO at a constant temperature of ∼350 °C. After the precursors were injected into the hot coordinating solvent (∼350 °C), the temperature of the growth solution was allowed to drop first to ∼300 °C and then to 150 °C by applying no further heat. The solution was then annealed at 150 °C for 15 min to ensure that the surface of the Qdots consisted of passivated TOPO/TOP. After the annealing was completed, the mixture was cooled to 70 °C. Next, *n*-butanol was added to the mixture to prevent the TOPO from solidifying upon cooling to room temperature. The products were extracted using a syringe, and were then recovered in powder form by precipitating them with methanol, and the precipitate was retrieved by centrifugation and redispersed in hexane, toluene and pyridine.

The 5.5 nm CdSe Qdots were produced through the secondary injection of different Cd, Se precursors. After the first injection, the secondary injection was performed by allowing the temperature of the extra precursors to drop slowly to growth temperature (290–300 °C). To obtain CdSe Qdots with a narrower size distribution, the process of redispersion of the precipitate in *n*-butanol followed by the size selective precipitation with methanol was repeated until no further sharpening of the optical absorption spectrum was noted. The precipitate obtained in this way was then redispersed in hexane.

2.3. Surface exchange

The precipitates of each type of CdSe Qdots were washed several times with methanol to remove excess ligands. The TOP/TOPO or TOPO/TDPA ligands on the surface of the Qdots were then replaced by refluxing the CdSe Qdots in pyridine (∼20 mL) under 1 atm of N_2 for 24 h. The Qdots were precipitated with hexanes at room temperature, recovered by centrifugation and dried for 3 min in a vacuum.

2.4. Preparation for hybrid solar cells

The typical procedure used to prepare the devices was as follows: indium tin oxide (ITO) glass was cleaned by successive ultrasonification with acetone, ethanol and millipore water for 30 min, respectively, followed by rinsing with DI water and blowing with nitrogen, and was then spin-coated onto PEDOT:PSS polymer. Following the spin-coating procedure, the films were heat-treated at 100 °C for 1 h under a vacuum. Photovoltaic devices were fabricated by spin-coating the CdSe Qdots–P3HT polymer solution and by spin-coating CdSe Qdots–MEH-PPV polymer solution containing a 1–8 vol.% pyridine–chloroform solvent mixture onto ITO under air. After spin-coating the Qdots–polymer solution on PEDOT:PSS polymer, the films were heat-treated at 100 °C for 30 min under a vacuum. Aluminum was used as the working electrode and was prepared by thermal evaporation. Fig. 1 shows the energy level diagram based on solar cells fabricated using P3HT (a) or MEH-PPV (b), in conjunction with the CdSe Qdots. Using these components, a sandwich type configuration was fabricated and the performance of the cell was measured. The solar cell was illuminated using a Xe lamp (Muller Elektronik Optik Inc., 500 W) and *I–V* measurements were obatined using an Autolab PGSTAT30 Potentiostat/Galvanostat.

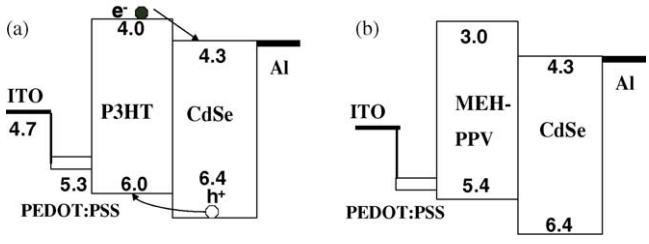

Fig. 1. (a) Energy level diagram of the CdSe Qdots and P3HT polymer device and (b) schematic diagram of the solar cells consisting of the CdSe Qdots and the MEH-PPV conjugated polymer (all numbers denote eV).

2.5. Measurement and characterization

The absorption spectra of the CdSe Qdots dispersed in *n*-hexane were obtained with a Hewlett–Packard 8452A diode-array UV–vis absorption spectrophotometer, and their luminescence properties were characterized by means of an ACTON spectrometer (SpectraPro-300i) connected with a photomultiplier tube (Acton Research, PD-438), using a xenon lamp connected to a monochrometer (SpectraPro-150i) as the excitation source. To identify and characterize the organic species on the surfaces, the Fourier transform infrared spectroscopy (FT-IR) spectra were obtained using a Perkin-Elmer Spectrum 2000. The structural properties of these organic species were confirmed by the powder X-ray diffraction (XRD) using a Rigaku rint 2000 model with a Cu Kα radiation source (1.5405 Å), X-ray photoelectron spectroscopy (XPS) using a VG-Scientific ESCALAB 250 spectrometer, SEM using a Hitachi S-4700 scanning electron microscope, and TEM using a Philips technai F20 electron microscope at 200 kV and a JEM 2010 electron microscope at 200 kV. The CdSe Qdots redispersed in hexane were dropped onto the thin amorphous carbon supported by a copper grid and dried at 60 °C in a vacuum for several hours. Further thin films of CdSe Qdots–P3HT polymer and CdSe Qdots–MEH-PPV blends with a thickness of approximately ∼100 nm were investigated using TEM, by spin-coating a film of the material on an NaCl IR window, floating the film in DI water, and picking it up with a copper TEM grid. Their morphological properties were also verified by using SEM using a Hitachi S-4700. After preparing each type of CdSe Qdots–P3HT polymer prepared in the form of a binary solvent mixture, we verified them by CV in order to measure the bandgap indirectly.

3. Results and discussion

3.1. Synthesis and characterization of CdSe Qdots

The size-controlled CdSe Qdots were yielded by varying the concentration of the Cd, Se precursors, the number of precursor injections and the growth temperature [12,16]. During the growth of each type of CdSe Qdots, the color of the solution gradually changed from colorless to reddish when the size of the Qdots attained 2.4 nm and to dark brown when their size attained 5.5 nm. This phenomenon was associated with the nuclei growth of the CdSe Qdots. When the precursors containing the Cd and Se powder were injected into the hot TOPO (∼350 °C) rapidly, the temperature of the mixture in the flask went abruptly down to 300–310 °C, then followed by slow cooling once the mantle was removed. We were able to deduce the variation in the growth rate over a certain time period.

Fig. 2(a) shows the optical properties of the CdSe Qdots in the formation of their absorption and luminescence spectra in *n*-hexane at room temperature. As the size of the CdSe Qdots increased, their optical properties varied and the wavelength range of the CdSe Qdots exhibited a red shift. These spectra showed a quantum confinement effect. The absorption spectra show an excitonic peak at from 465 to 610 nm. The luminescence spectra from 490 to 620 nm are shown in Fig. 2(a). The high quantum yields and narrow emission line widths of the Qdots were attributed to the presence of relatively few defect sites in the CdSe Qdots. Fig. 2 shows HRTEM images of the CdSe Qdots with sizes of (b) 2.4 nm (538/555 nm), (c) 3.6 nm (569/574 nm) and (d) 5.5 nm (610/620 nm at UV–vis/PL), which show the crystalline structure of the CdSe Qdots, respectively.

FT-IR spectroscopy in Fig. 3 was used to identify and characterize the organic species present on the surface of the CdSe Qdots. Fig. 3 shows the FT-IR spectrum of the CdSe Qdots in *n*-hexane, which might be the surface termination of these particles by methyl groups whose presence is shown by the peaks at 2853, 2927 and 2965 cm^{-1}. On the basis of the FT-IR data, the surface of the CdSe Qdots is mainly coated with alkyl ligands. Flexible organic molecules such as methyl or phosphine alkyl ligands provide repulsive interactions between the Qdots in *n*-hexane, thus preventing aggregation. Others show 3417 cm^{-1} at –OH, 2360 cm^{-1} at $-PH_3$, 1464 cm^{-1} at $-CH_2$, 1155 cm^{-1} at –P=O functional group, and fingerprint range at remain wavenumber, respectively. Fig. S1 shows the results for Cd and Se using XPS, which were obtained for the 5.5 nm CdSe Qdots. The XPS of 5.5 nm CdSe Qdots show the representive Se $3d_{5/2}$, Cd $3d_{5/2}$ peaks. The condition of scan width of narrow scan spectrum at 0.05 eV, scan width of wide scan spectrum at 1 eV and binding energy of C_{1S} ∼284.6 eV estimated. The binding energy of Cd element of CdSe Qdots is $3d_{5/2} = 405.1$, $3d_{3/2} = 411.89$ and $\Delta = 6.79$ eV. The energy shift of Cd element compared with the Handbook of XPS spectroscopy was less shifted. The binding energy of Se element of CdSe Qdots is $3d_{5/2} = 53.6$, $3d_{3/2} = 54.2$ and $\Delta = 0.6$ eV. Comparing with the Handbook of XPS spectroscopy, the energy shift of Se element was $3d_{5/2} = 2$, $3d_{3/2} = 2.8$ and $\Delta = 0.8$ eV. The existence of the contaminants was not identified. Further, we analyzed CdSe Qdots characteristics using other analysis tools. Therefore, the XPS results provide an enough evidence for the chemical surface states of the CdSe Qdots.

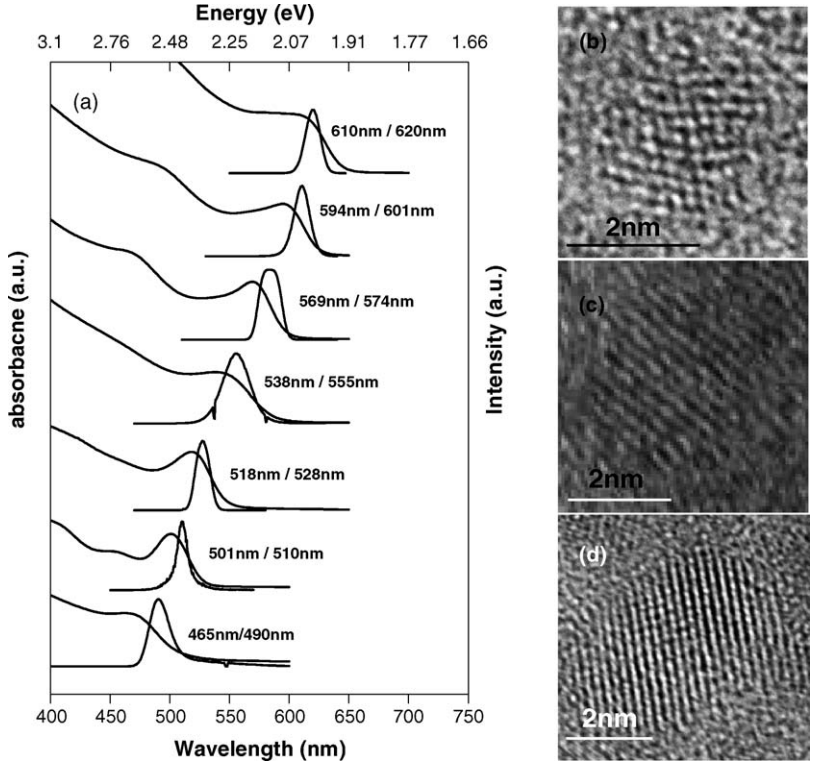

Fig. 2. (a) UV–vis spectra and PL spectra of the size-controlled CdSe Qdots. HRTEM images of (b) 2.4 nm, (c) 3.6 nm and (d) 5.5 nm CdSe Qdots.

The XRD patterns of the CdSe Qdots is shown in Fig. 4. These particle sizes, which were based on the Scherer formular analysis of the peak widths, were obtained from the FWHM of the (1 1 0) peak, because the CdSe Qdots with (1 1 0) spacing have a wurtzite structure according to the JCPD No. 08–0456. In Fig. S2, the TEM image of the CdSe Qdots revealed that these spherical CdSe Qdots have an average diameter of 5.5 nm, as shown in the histogram in Fig. S2(b). Some researchers mentioned that the HRTEM image of a single Qdots revealed the presence of an atomic lattice fringe, demonstrating the crystalline structure of the nanocrystallites. The CdSe Qdots have a wurtzite crystal structure, as confirmed by the electron diffraction pattern shown in Fig. S2(a, inset). The particle size calculated from the Scherer formula matched very well with the TEM data. The CdSe Qdots with an average diameter of 5.5 nm were slightly elongated particles with aspect ratios of between 1.1 and 1.3 toward the *c*-axis dimension. This ability to the size-controlled of CdSe Qdots allowed them to have desirable characteristics from the viewpoint of their potential applications.

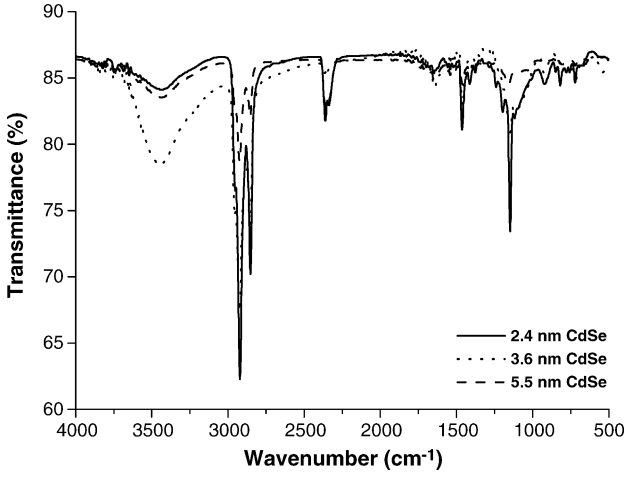

Fig. 3. FT-IR spectrum of the 2.4 (solid), 3.6 (dot) and 5.5 nm (dash line) CdSe Qdots in *n*-hexane.

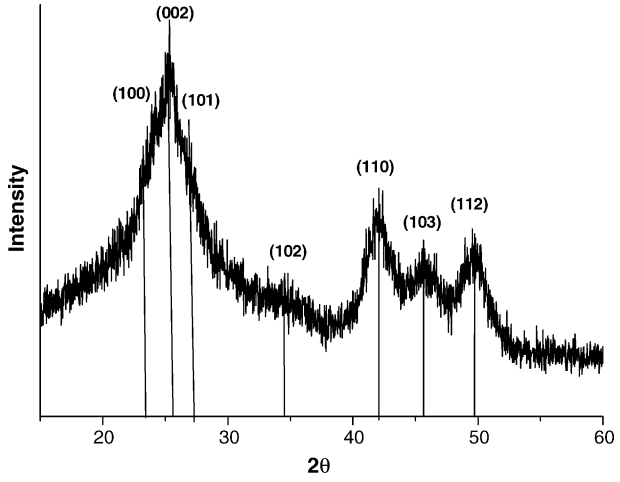

Fig. 4. Powder XRD pattern of the 5.5 nm CdSe Qdots.

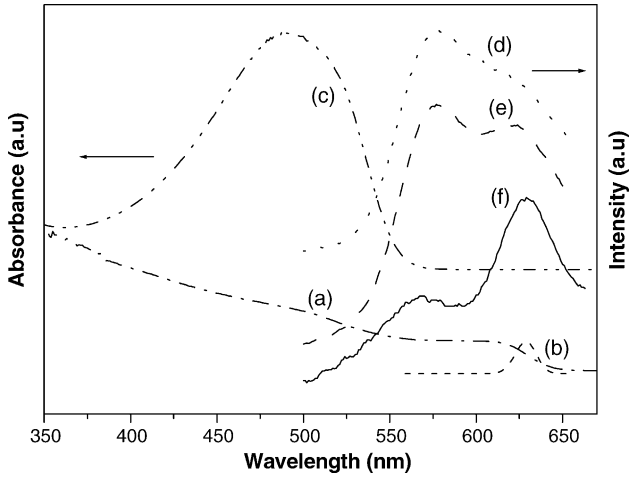

Fig. 5. The CdSe Qdots–MEH-PPV polymer blends; (a) absorption spectra of CdSe Qdots, (b) PL of CdSe QDots, (c) absorption spectra of MEH-PPV, (d) PL of MEH-PPV, (e) PL of 50 wt.% CdSe Qdots–MEH-PPV blends and (f) PL of 90 wt.% CdSe Qdots–MEH-PPV blends.

3.2. Hybrid CdSe Qdots–conjugated polymer solar cells

Fig. 5 shows the absorption spectra and luminescence spectra of blending the 5.5 nm CdSe Qdots–MEH-PPV polymer at room temperature with an excitation of 480 nm. As wt.% CdSe Qdots concentration increased, the luminescence of unique MEH-PPV polymer decreased. Our finding that strong luminescence peak of 576 nm MEH-PPV (Fig. 5(d)) decrease while the luminescence at 625 nm at 90 wt.% concentration of CdSe Qdots (Fig. 5(f)) increased, relatively. In the Fig. 5(a and b), the absorption spectra of CdSe Qdots and the luminescence of spectra have 610 and 625 nm, respectively. The absorption spectra of MEH-PPV polymer show in Fig. 5(c). Fig. 5(e) shows at 50 wt.% CdSe Qdots–polymer blending. These results indicate that the charge transfer occurred between the MEH-PPV polymer and the CdSe Qdots.

We were able to enhance the efficiency of the device through the use of a binary solvent mixture. The aim of this procedure was to enhance the solubility of the CdSe Qdots by using a good solvent and by exchanging the ligands on the surface of the CdSe Qdots. Thus, we selected a combination of pyridine and chloroform as the solvent. Since pyridine disperses in chloroform, there is a resultant solubility increase for the CdSe Qdots. To investigate the morphology of 5.5 nm CdSe Qdots–polymer films in this binary solvent mixture, we estimated TEM images to study the morphology.

Fig. 6(a and c) show TEM images of P3HT/TOPO-coated CdSe Qdots blends and Fig. 6(b and d) show TEM images of surface exchanged P3HT/pyridine-coated CdSe Qdots blends in various CdSe Qdots concentration. Fig. S3(a and c) show TEM images of MEH-PPV/TOPO-coated CdSe Qdots blends and Fig. S3(b and d) show TEM images of MEH-PPV/pyridine-coated CdSe Qdots blends. It is

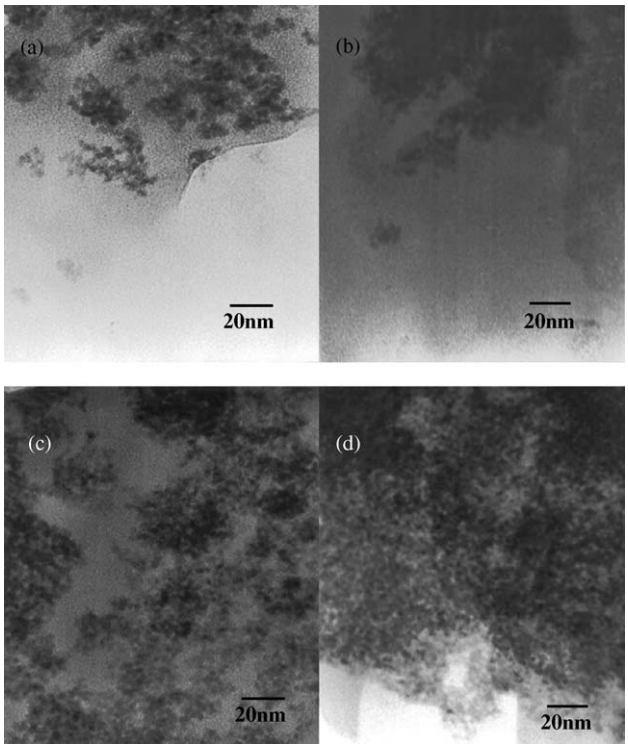

Fig. 6. TEM images of P3HT/5.5 nm CdSe Qdots blends; (a and c) P3HT/TOPO-coated CdSe Qdots, (b and d) P3HT/pyridine-treated CdSe Qdots in 20 wt.% (a and b) and 90 wt.% (c and d) concentration of CdSe Qdots.

shown that even in the case of the 20 wt.% blends, the CdSe Qdots aggregated together to form predomain regions of densely packed nanocrystals surrounded by regions of polymer. As the concentration of Qdots is increased, the densely packed Qdots aggregate together increasingly. TEM images of polymer in pyridine-coated CdSe Qdots blends show that the driving force for phase segregation seems to be the difference of polarity between the relative polar pyridine-coated CdSe Qdots and the relative non-polar polymer. TEM images of polymer in TOPO-coated CdSe Qdots blends show that this aggregation seems to be driven by van der waals interactions between the CdSe Qdots. With these reasons, the pyridine-coated CdSe Qdots blends are more aggregate than the TOPO-coated CdSe Qdots blends [4,10,11].

Fig. S4 shows the SEM images and EDX analysis which show the difference in morphology between the CdSe Qdots and conjugated polymer, in the case of P3HT (a–f) and MEH-PPV (g–l) containing 0 wt.% (a and g), 20 wt.% (b and h), 50 wt.% (d and j) and 90 wt.% (e and k) CdSe Qdots, treated with pyridine for the surface-exchanged purpose. This figure also shows the SEM image of the 90 wt.% TOPO-coated CdSe Qdots–MEH-PPV polymer blends (l) and EDX analysis shown in Fig. S4(c and i). The SEM image was taken after blending of the CdSe Qdots–P3HT, the CdSe Qdots–MEH-PPV polymer on Si substrate, respectively. The EDX results confirmed the element of Cd and Se (atomic ratio = about

1:1), respectively. Thus, CdSe Qdots tend to form much bigger aggregates than the domain of CdSe Qdots. Because the phase segregation phenomenon and van der waals interactions improve as the contact area between the aggregating particles increases, there is a tendency for the CdSe Qdots to aggregate would be occurred [17]. Fig. S4(f) shows the cross sectional image of various CdSe Qdots–P3HT polymer blends based on the solar cell devices. The AFM images in Fig. S5 show the CdSe Qdots–P3HT, and CdSe Qdots–MEH-PPV blends. 3D image and morphology are the CdSe Qdots–conjugated polymer that P3HT (a, inset) and MEH-PPV (b, inset) contained 50 wt. % CdSe Qdots with 8 vol.% pyridine–chloroform as in a binary solvent mixture. Root mean square (RMS) of CdSe Qdots–conjugated polymer blends increased with more wt.% CdSe Qdots concentration.

Furthermore, we applied the fabrication of solar cells as charge transport occurred between the CdSe Qdots and P3HT polymer. CdSe Qdots are used as the electron transport material. The P3HT polymer is an effective hole transport material, exhibiting the highest field effect hole mobility observed in polymers so far, with a value of up to 10^{-2} $cm^2/(V\,s)$ [18]. The device structure consists of a film ~270 nm (approximately Al ~100 nm, CdSe/P3HT or MEH-PPV blends ~100 nm, PEDOT:PSS ~70 nm) in thickness sandwiched between an aluminum electrode and a transparent conducting electrode made of PEDOT:PSS deposited on an ITO glass substrate. However, the morphology of the films is not yet optimized for charge transfer due to the pronounced clustering of the materials.

Fig. 7(a) shows the *I–V* curve for the photovoltaic cell made from a each composite, consisting of the 5.5 nm CdSe Qdots–P3HT polymer and 5.5 nm CdSe Qdots–MEH-PPV polymer under A.M. 1.5 global solar conditions. A maximum power conversion efficiency of about 0.05%, an open circuit voltage of 1.00 V, a short-circuit current density of 2.16 $\mu A/cm^2$, and a fill factor of 0.20 were obtained in the photovoltaic device which consisted of the P3HT polymer with 90 wt.% CdSe Qdots. In the case of the CdSe Qdots–polymer composite, the I_{sc} was decreased with increasing time and the degradation was reduced using the PEDOT:PSS/CdSe Qdots–polymer electrodes.

Incident photon-to-current conversion efficiency (IPCE) was measured using the same cells as used in the *I–V* curve measurements. Under the controlled light illumination, the steady-state current density was measured by means of potentiostat and this value was shown in Fig. 7(b). Fig. 7(b) shows photocurrent density for hybrid solar cells using a PEDOT/90 wt.% 5.5 nm CdSe Qdots–MEH-PPV polymer electrode (filled circles) and a PEDOT/90 wt.% 5.5 nm CdSe Qdots–P3HT polymer electrode (filled reverse triangle), respectively. The photocurrent density was determined at the short-circuit state. The improved photocurrent density due to the reduced recombination rate was observed by PEDOT conducting polymer in the fabrication of the hybrid solar cells. Due to the existence of conducting polymer layer,

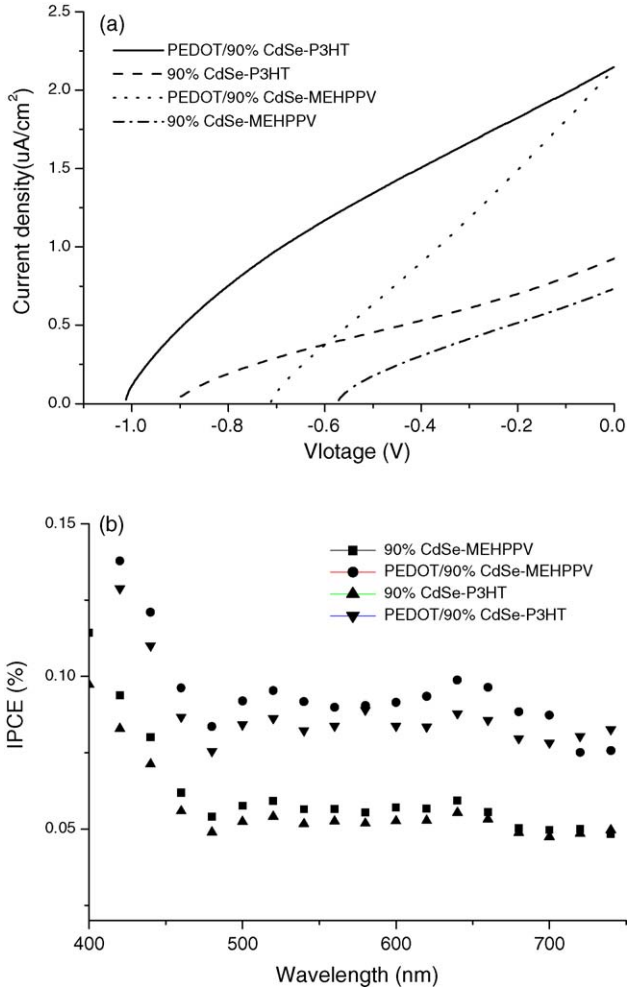

Fig. 7. The 5.5 nm CdSe Qdots–P3HT blends and the 5.5 nm CdSe Qdots–MEH-PPV polymer blends used for the hybrid solar cells under A.M. 1.5 global solar conditions; (a) *I–V* curve (0.05% of PEDOT:CdSe Qdots–P3HT, 0.01% without PEDOT, 0.02% of PEDOT:CdSe Qdots–MEH-PPV, 0.005% without PEDOT) and (b) wavelength dependence of photocurrent density for hybrid solar cells.

CdSe Qdots, MEH-PPV, P3HT polymer, improvement of IPCE can be expected.

It presumes that insufficient results may be due to these reasons as follows. These reasons can be attributed to several different causes: (1) a decrease in the recombination rate, (2) the stability of the adsorbed CdSe Qdots while they are illuminated, (3) the charge transport limitation between the CdSe Qdots and the polymer, (4) a vague mechanism of interfacial electron or hole formation between the CdSe Qdots and polymer [10,11,19]. Our finding the surface deep traps, low carrier mobility and the incomplete surface exchange of the CdSe Qdots may not be accomplished by improving the interface between the CdSe Qdots and polymer. Furthermore, we may reconsider the ohmic contact problem of fabrication as hybrid solar cells. Although Huynh et al. [5,6] showed higher conversion efficiency of hybrid solar cells, we would like to focus on the above parameters in order to develop

hybrid solar cells with the modified size-controlled CdSe Qdots.

4. Conclusion

The size-controlled CdSe Qdots are synthesized by using the wet chemical synthetic method. We obtained the optical properties using the absorption and PL spectra of the CdSe Qdots. We also confirmed the structural properties of the CdSe Qdots by XPS, SEM, XRD and TEM, and characterized the CdSe Qdots–conjugated polymer blends. The hybrid solar cells made of CdSe Qdots–P3HT polymer blends with the pyridine–chloroform solvent mixture could achieve power conversion efficiencies of about 0.05% under A.M. 1.5 global solar conditions. Although we did not attain sufficient power conversion efficiency under Huynh et al. [5], we synthesized the size-controlled CdSe Qdots with the modified method, which could be applied to the fabrication of solar cells. We confirmed that binary solvent mixtures play an important role in the fabrication of hybrid inorganic semiconductors and conjugated polymer blends, which are used for electronic applications because they are used to produce the Qdots in the exchanged surface of the organic surfactants. Therefore, it needs further works to obtain the improved performance of photovoltaic cells solving problems of the physical respects.

Acknowledgements

This work was supported by KOSEF through the Research Center for Energy Conversion and Storage and Grant No. R01-2004-000-10143 in Korea. We also wish to thank MOST and the Center for CNNC for the funding which they provided.

Appendix A. Supplementary data

Supplementary data associated with this article can be found, in the online version, at doi:10.1016/j.jphotochem.2005.08.004.

References

[1] C.J. Brabec, N.S. Sariciftci, J.C. Hummelen, Adv. Funct. Mater. 11 (2001) 15.
[2] C.W. Tang, Appl. Phys. Lett. 48 (1986) 183.
[3] M. Granström, K. Petritsch, A.C. Arias, A. Lux, M.R. Andersson, R.H. Friend, Nature 395 (1998) 257.
[4] B. O'Regan, M. Grätzel, Nature 353 (1991) 737.
[5] W.U. Huynh, J.J. Dittmer, A.P. Alivisatos, Science 295 (2002) 2425.
[6] W.U. Huynh, J.J. Dittmer, W.C. Libby, G.L. Whitting, A.P. Alivisatos, Adv. Funct. Mater. 13 (2003) 73.
[7] S.E. Shaheen, et al., Appl. Phys. Lett. 78 (2001) 841.
[8] G. Yu, J. Gao, J.C. Hummelen, F. Wudl, A.J. Heeger, Science 270 (1995) 1789.
[9] J.J. Dittmer, E.A. Marseglia, R.H. Friend, Adv. Mater. 12 (2000) 1270.
[10] N.C. Greenham, X. Peng, A.P. Alivisatos, Phys. Rev. B 54 (1996) 17628.
[11] D.S. Ginger, N.C. Greenham, Phys. Rev. B 59 (1999) 10622.
[12] C.B. Murray, D.J. Norris, M.G. Bawendi, J. Am. Chem. Soc. 115 (1993) 8709.
[13] K. Rajeshwar, N.R. de Tacconi, C.R. Chenthamarakshan, Chem. Mater. 13 (2001) 2765.
[14] M. Kolosky, J. Vlalle, T. Cotel, J. Chromatogr. 299 (1984) 436.
[15] F. Wudl, US Patent 1990 No. 5189136, Chem. Abstr. 118 (1993) 255575.
[16] A.H. Margaret, G.S. Phillippe, J. Phys. Chem. 100 (1996) 468.
[17] P.C. Ohara, D.V. Leff, J.R. Heath, W.M. Gelbart, Phys. Rev. Lett. 75 (1995) 3466.
[18] H. Sirringhaus, N. Tessler, R.H. Friend, Science 280 (1998) 1741.
[19] S.S. Kim, J.H. Yum, Y.E. Sung, Sol. Energy Mater. Sol. Cells 79 (2003) 495.